

Total Structure Determination of Thiolate-Protected Au₃₈ Nanoparticles

Huifeng Qian,[†] William T. Eckenhoff,[‡] Yan Zhu,[†] Tomislav Pintauer,[‡] and Rongchao Jin^{*†}

Department of Chemistry, Carnegie Mellon University, Pittsburgh, Pennsylvania 15213 and Department of Chemistry and Biochemistry, Duquesne University, Pittsburgh, Pennsylvania 15282

Received May 3, 2010; E-mail: rongchao@andrew.cmu.edu

We previously reported the crystal structures of ultrasmall, 25-gold-atom [Au₂₅(SC₂H₄Ph)₁₈]^q (*q* = −1, 0) nanoparticles (also called nanoclusters).^{1,2} Herein we extend our effort to the case of 38-atom Au₃₈ nanoparticles. In our previous crystallization work, we found that the purity of nanoparticles is critical; thus, our significant effort in Au₃₈ nanoparticles has been focused on synthesizing atomically monodisperse Au₃₈ nanoparticles.³ The Au₃₈ nanoparticles pertain to the ~8 kDa species earlier reported by Schaaff et al.⁴ A formula of Au₃₈(SC₆H₁₃)_{23–24} was suggested by Whetten et al. based upon XPS measurements,⁵ but at that time the exact formula was not confirmed by mass spectrometry, for that laser desorption ionization (LDI) MS analysis often results in fragmentation of the particles, which complicates the formula determination.⁶ Recently, Chaki et al. reported isolation and electrospray ionization (ESI) MS analysis of Au₃₈(SC₁₂H₂₅)₂₄, but the yield was quite low.⁷ We have been able to improve the synthetic method and largely increased the yield of Au₃₈(SC₁₂H₂₅)₂₄ to ~10%, and the Au₃₈(SC₁₂H₂₅)₂₄ composition was verified by LDI-MS, ESI-MS, and other characterization.^{3a} A particular advantage of our method lies in that it eliminates nontrivial postsynthetic separation steps involved in previous work by Chaki.⁷ Very recently, we have further improved the method and synthesized truly monodisperse, phenylethylthiolate capped Au₃₈(SC₂H₄Ph)₂₄ nanoparticles (yield ~25%),^{3b} which opens up the possibility of crystallization trials.

In this work, we have prepared Au₃₈(SC₂H₄Ph)₂₄ nanoparticles with molecular purity following the synthetic method^{3b} reported recently. These atomically monodisperse nanoparticles were then crystallized in a mixed solution of toluene and ethanol, similar to our previous work of [Au₂₅(SC₂H₄Ph)₁₈]^q (*q* = −1, 0). Dark crystals were collected, and the structure of Au₃₈(SC₂H₄Ph)₂₄ was determined by X-ray crystallography.

The Au₃₈(SR)₂₄ (R = C₂H₄Ph) crystal structure has a triclinic space group *P* $\bar{1}$. Interestingly, the unit cell contains a pair of enantiomeric nanoparticles. Both isomers show a prolate shape resembling a nanorod. To find out details of the atom packing structure, we choose the left handed isomer for a detailed analysis. Figure 1 shows the total structure of the left handed Au₃₈(SR)₂₄ nanoparticle. The nanoparticle is based on a face-fused biicosahedral Au₂₃ core, which is capped by a second shell comprised of the rest 15 gold atoms, hence, a core–shell structure. If one takes the thiolate ligands into consideration, the particle may also be viewed as a Au₂₃ core plus three monomeric staples (RS–Au–SR, abbreviated as Au(SR)₂ below) and six dimeric staples (RS–Au–S(R)–Au–SR, abbreviated as Au₂(SR)₃ below). A similar structure was discussed by Pei et al. in DFT calculations.⁸

An anatomy of the total structure better starts with a centered icosahedron Au₁₃ (Figure 2). A Au₁₃ icosahedron possesses C₅, C₃, and C₂ rotation axes. Figure 2 (left) shows a view along the C₃

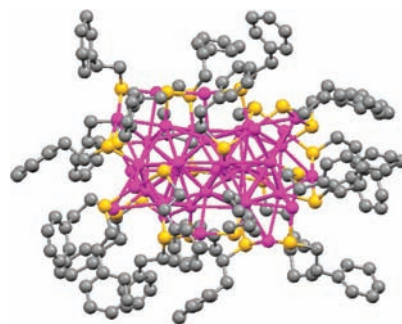


Figure 1. Total structure of Au₃₈(SC₂H₄Ph)₁₈ (L-isomer, color labels: magenta, Au; yellow, S; gray: C, H atoms are omitted).

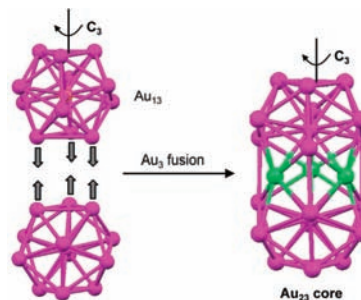


Figure 2. Anatomy of the Au₂₃ core structure of Au₃₈(SC₂H₄Ph)₂₄.

axis; in this view, the icosahedron is composed of a top Au₃ face and a bottom one as well as a Au₆ corrugated plane (“chair”) in between the two Au₃ faces. When two icosahedra are fused together via sharing a common Au₃ face, one obtains face-fused biicosahedral Au₂₃ (i.e., 13 × 2 − 3 = 23), which constitutes the core of the Au₃₈(SR)₂₄ nanoparticle. In either unit of the dimeric Au₂₃ core, bond lengths between the central atom and the first-shell Au atoms range from 2.76 to 2.84 Å, while the Au–Au distance at the shell (excluding Au atoms in the fusion plane) is 2.76–3.08 Å. Within the fusion plane, Au–Au bond distances are significantly longer (average 3.28 Å). Between the two Au₆ corrugated planes, three nearest Au–Au pairs show bond lengths of average 3.0 Å and are evenly distributed at the waist of the Au₂₃ rod (Figure 2, right). The Au₂₃ core adopts a quasi-*D*_{3h} symmetry.

The exterior Au shell comprises 15 Au atoms face-capped onto the Au₃ faces of the Au₂₃ core; note that some Au₃ faces are left uncapped. Each exterior Au atom has one shorter Au–Au contact (3.04–3.12 Å) to the biicosahedron and two longer ones (3.18–3.29 Å) to the other two Au atoms on the Au₃ face it is capping. At the Au₃ fusion plane, three exterior shell Au atoms are respectively bonded to the three Au atoms of the fusion plane in a radial fashion, and the average Au–Au distance is 3.0 Å. The face-fused biicosahedral Au₂₃ core is quite remarkable and is reminiscent of previous work of vertex-sharing [Au₂₅(PPh₃)₁₀(SC₂H₅)₅Cl₂]²⁺

[†] Carnegie Mellon University.

[‡] Duquesne University.

reported by Tsukuda et al.⁹ and vertex-sharing Au/Ag phosphine nanoclusters by Teo et al.,¹⁰ such as biicosahedral $[\text{Au}_{13}\text{Ag}_{12}(\text{PPh}_3)_{10}\text{Br}_8]^+$, triicosahedral $\text{Au}_{18}\text{Ag}_{20}(\text{ToI}_3\text{P})_{12}\text{Cl}_{14}$, and tetraicosahedral $\text{Au}_{22}\text{Ag}_{24}(\text{Ph}_3\text{P})_{12}\text{Cl}_{10}$. The face-fused biicosahedral Au_{23} rod is indeed for the first time observed in $\text{Au}_{38}(\text{SR})_{24}$. It is worth noting that an interpenetrated triicosahedral Pd_{23} core was previously reported by Mednikov and Dahl in $\text{Pd}_{37-38}(\text{CO})_{28-29}[\text{P}(p\text{-Tolyl})_3]_{12}$ nanoclusters.¹¹

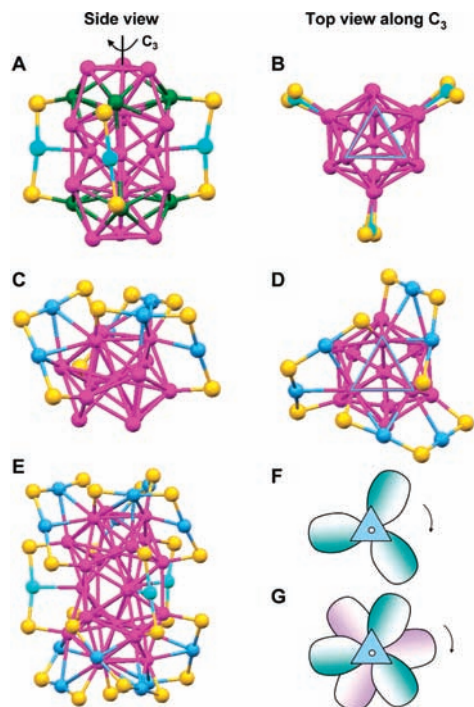


Figure 3. Anatomy of the surface structure of $\text{Au}_{38}(\text{SC}_2\text{H}_4\text{Ph})_{24}$. (A, C, E) Side views; (B, D) Top view; (F, G) Geometric models; see text for detailed explanations. For clarity, $\text{CH}_2\text{CH}_2\text{Ph}$ is omitted. Color labels: yellow, S; all the other colors are for Au atoms in different positions.

If the thiolate ligands are taken into consideration, the $\text{Au}_{23}/\text{Au}_{15}$ core-shell structure may also be viewed as a Au_{23} core protected by three monomeric $\text{Au}(\text{SR})_2$ staples and six dimeric $\text{Au}_2(\text{SR})_3$ staples (hence, $3 \times 1 + 6 \times 2 = \text{Au}_{15}$ shell). The three $\text{RS}-\text{Au}-\text{SR}$ monomeric staples bridge the two Au_6 corrugated planes by stapling the three farthest $\text{Au}-\text{Au}$ pairs (~ 5.3 Å), respectively, Figure 3A–B (top and side views); note that the three nearest pairs form direct $\text{Au}-\text{Au}$ contacts (~ 3 Å) as aforementioned. Also as discussed above, the three Au atoms in the monomeric staples form direct bonds with the Au_3 fusion plane (Figure 3A) with an average bond distance of ~ 3.00 Å; thus, one could view the three $\text{Au}(\text{SR})_2$ staples to strengthen the two fused Au_{13} units. The $(\text{R})\text{S}-\text{Au}-\text{S}(\text{R})$ is nearly linear (average bond angle $\sim 168.6^\circ$), and the average $\text{Au}-\text{S}$ bond length is 2.30 Å. As for the six “V”-shaped $\text{RS}-\text{Au}-\text{S}(\text{R})-\text{Au}-\text{SR}$ dimeric staples, three are distributed on the top icosahedron and the other three on the bottom Au_{13} unit. To observe details of the arrangement of the $\text{Au}_2(\text{SR})_3$ staples, the top icosahedron with three $\text{Au}_2(\text{SR})_3$ staples is shown in Figure 3C–D (side and top views, respectively). Apparently, the arrangement resembles a triblade fan (Figure 3F) with C_3 as the axis. The average $\text{Au}-\text{S}(\text{R})-\text{Au}$ angle in the dimeric staples is $\sim 102.7^\circ$. As for the bottom portion of the $\text{Au}_{38}\text{S}_{24}$ framework, the same triblade fan configuration is observed (Figure 3E), but the bottom fan rotates $\sim 60^\circ$ relative to the top fan; hence, the top and bottom fans exhibit a staggered configuration (Figure 3G). Both triblade fans rotate clockwise (or left-handed) for this stereoisomer.

The right-handed isomer possesses the same Au_{23} core, but the six dimeric staples rotate counter-clockwise. Therefore, the chirality of $\text{Au}_{38}(\text{SR})_{24}$ nanoparticles¹² originates from the Au_{15} shell, rather than from the rod-shaped Au_{23} core as the latter possesses symmetry planes (D_{3h}).

No counterion is found in the unit cell, which indicates that the $\text{Au}_{38}(\text{SC}_2\text{H}_4\text{Ph})_{24}$ nanoparticle is charge neutral. This is consistent with NMR analysis, in which only phenylethyl (^1H) signals were found. Elemental analysis also supports this conclusion, in which only C, H, S were found (no N or other nonmetal elements).

It is worthy of a comparison of the $\text{Au}_{38}(\text{SR})_{24}$ X-ray structure with those theoretical structures.^{8,13–15} A number of structures with a symmetric or disordered Au core were previously predicted by Hakkinen, Garzon, Tsukuda, Jiang, and Zeng et al.^{7,8,13–15} Tsukuda et al. discussed several possibilities of the core and staple motifs based upon some empirical structural rules.⁷ Among the theoretical structures, the model computed by Zeng et al.⁸ is indeed quite close to the X-ray structure of $\text{Au}_{38}(\text{SR})_{24}$. However, the arrangement of the dimeric staples on the icosahedral Au_{13} unit was not correctly predicted; in the theoretical structure, the six dimeric staples distributed on two icosahedra have a mirror plane (i.e., the Au_3 fusion plane), but the crystal structure shows that the six dimeric staples are arranged in a staggered fashion (Figure 3G) with an inversion center in the fused plane.

In summary, this work reports the crystal structure of $\text{Au}_{38}(\text{SR})_{24}$ nanoparticles. This constitutes an important step toward understanding the electronic, optical, and other interesting properties of $\text{Au}_{38}(\text{SR})_{24}$ nanoparticles. With more structures determined by X-ray crystallography, the evolution of $\text{Au}_n(\text{SR})_m$ nanoparticles from molecule-like clusters to face-centered cubic (fcc) nanocrystals will be ultimately understood.¹⁶

Acknowledgment. We thank Dr. F. J. Hollander, Dr. A. DiPasquale, and Dr. S. Geib for assistance and helpful discussions and Prof. C. M. Aikens for sending us a manuscript on the prediction of chirality and structure of $\text{Au}_{38}(\text{SCH}_3)_{24}$. This work is financially supported by CMU, DU, AFOSR, and NIOSH.

Supporting Information Available: Detailed information about X-ray analysis of $[\text{Au}_{38}(\text{SCH}_2\text{CH}_2\text{Ph})_{24}]^0$. This material is available free of charge via the Internet at <http://pubs.acs.org>.

References

- Zhu, M.; Aikens, C. M.; Hollander, F. J.; Schatz, G. C.; Jin, R. *J. Am. Chem. Soc.* **2008**, *130*, 5883.
- Zhu, M.; Eckenhoff, W. T.; Pintauer, T.; Jin, R. *J. Phys. Chem. C* **2008**, *112*, 14221.
- (a) Qian, H.; Zhu, M.; Andersen, U. N.; Jin, R. *J. Phys. Chem. A* **2009**, *113*, 4281. (b) Qian, H.; Zhu, Y.; Jin, R. *ACS Nano* **2009**, *3*, 3795.
- (a) Schaaff, T. G.; Shafiqullin, M. N.; Khoury, J. T.; Vezmar, I.; Whetten, R. L.; Cullen, W. G.; First, P. N.; Gutierrez-Wing, C.; Ascensio, J.; Jose-Yacamán, M. J. *J. Phys. Chem. B* **1997**, *101*, 7885–7891. (b) Schaaff, T. G.; Whetten, R. L. *J. Phys. Chem. B* **1999**, *103*, 9394–9396.
- Hakkinen, H.; Barnett, R. N.; Landman, U. *Phys. Rev. Lett.* **1999**, *82*, 3264.
- Toikkanen, O.; Ruiz, V.; Ronholm, G.; Kalkkinen, N.; Liljeroth, P.; Quinn, B. M. *J. Am. Chem. Soc.* **2008**, *130*, 11049.
- Chaki, N. K.; Negishi, Y.; Tsunoyama, H.; Shichibu, Y.; Tsukuda, T. *J. Am. Chem. Soc.* **2008**, *130*, 8608.
- Pei, Y.; Gao, Y.; Zeng, X. C. *J. Am. Chem. Soc.* **2008**, *130*, 7830.
- Shichibu, Y.; Negishi, Y.; Watanabe, T.; Chaki, N. K.; Kawaguchi, H.; Tsukuda, T. *J. Phys. Chem. C* **2007**, *111*, 7845.
- Teo, B. K.; Zhang, H. *Coord. Chem. Rev.* **1995**, *143*, 611.
- Mednikov, E. G.; Dahl, L. F. *J. Am. Chem. Soc.* **2008**, *130*, 14813.
- Schaaff, T. G.; Whetten, R. L. *J. Phys. Chem. B* **2000**, *104*, 2630.
- Hakkinen, H.; Walter, M.; Gronbeck, H. *J. Phys. Chem. B* **2006**, *110*, 9927.
- (a) Jiang, D.; Tiago, M. L.; Luo, W.; Dai, S. *J. Am. Chem. Soc.* **2008**, *130*, 2777. (b) Jiang, D.; Luo, W.; Tiago, M. L.; Dai, S. *J. Phys. Chem. C* **2008**, *112*, 13905.
- Garzon, I. L.; Reyes-Nava, J. A.; Rodriguez-Hernandez, J. I.; Sigal, I.; Beltran, M. R.; Michaelian, K. *Phys. Rev. B* **2002**, *66*, 073403.
- Jin, R. *Nanoscale* **2010**, *2*, 343.

JA103592Z